

## SUPPLEMENTARY INFORMATION

### Roles of Transition Metals Interchanging with Lithium in Electrode Materials

Tomoya Kawaguchi,<sup>1</sup> Katsutoshi Fukuda,<sup>2</sup> Kazuya Tokuda,<sup>1</sup> Masashi Sakaida,<sup>1</sup> Tetsu

Ichitsubo,<sup>1</sup> Masatsugu Oishi,<sup>3</sup> Jun'ichiro Mizuki,<sup>4</sup> and Eiichiro Matsubara<sup>1</sup>

<sup>1</sup>*Department of Materials Science and Engineering, Kyoto University, Kyoto 606-8501, Japan*

<sup>2</sup>*Office of Society-Academia Collaboration for Innovation, Kyoto University, Kyoto*

*611-0011, Japan*

<sup>3</sup>*Graduate School of Engineering, Kyoto University, Kyoto 606-8501, Japan*

<sup>4</sup>*School of Science and Technology, Kwansei Gakuin University, Hyogo 669-1337, Japan*

#### Rietveld analyses of the electrode materials

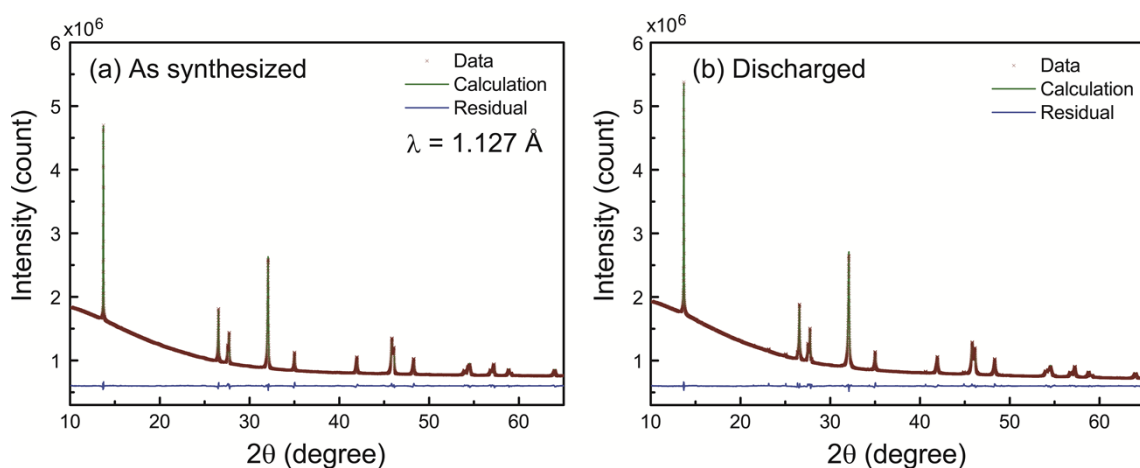


Figure S1. The resultant XRD profiles of the Rietveld analyses of (a) as-synthesized and (b) discharged samples. Symbols indicate the experimental values. Green and blue solid lines represent the simulated curve and the residual of the fitting, respectively. The XRD profiles were

obtained by the Debye-Scherrer method using a two-dimensional detector.

Table S1. Refined structural parameters obtained from the Rietveld analyses. A hexagonal structure (space group No. 166,  $R\bar{3}m$ ) was used for the fitting. The  $R$  values indicating the goodness of fit were  $R_{wp} = 0.511$ ,  $S = 5.11$  and  $R_{wp} = 0.520$ ,  $S = 5.26$  for the as-synthesized and discharged samples, respectively.

Sample	Lattice constants (Å)		Element	Site	$g^d$	$x$	$y$	$z$	$B^e$	Constraint
	a	c								
As synthesized	2.87837(10)	14.1891	Li <sup>+</sup>	3a	0.8936	0	0	0	1.5	$g = 1 - g(\text{Ni}^{3+}@3a)$
			Ni <sup>3+</sup>	3a	0.1064(4)	0	0	0	0.485(8)	
			Ni <sup>3+</sup>	3b	1.0	0	0	0.5	0.485	$B = B(\text{Ni}^{3+}@3a)$
			O <sup>2-</sup>	6c	1.0	0	0	0.24198(5)	0.93(18)	
Discharged <sup>f</sup>	2.87546(12)	14.2159	Li <sup>+</sup>	3a	0.77	0	0	0	1.5	
			Ni <sup>3+</sup>	3a	0.1077(4)	0	0	0	0.938(8)	
			Ni <sup>3+</sup>	3b	1.0	0	0	0.5	0.938	$B = B(\text{Ni}^{3+}@3a)$
			O <sup>2-</sup>	6c	1.0	0	0	0.24108 (5)	1.55(18)	

<sup>d</sup> $g$  denotes occupancy of atoms.

<sup>e</sup> $B$  is the Debye-Waller factor.

<sup>f</sup>The bond length of Li-O was determined to be 2.1157 Å from the obtained structural parameters.

### DAFS spectra

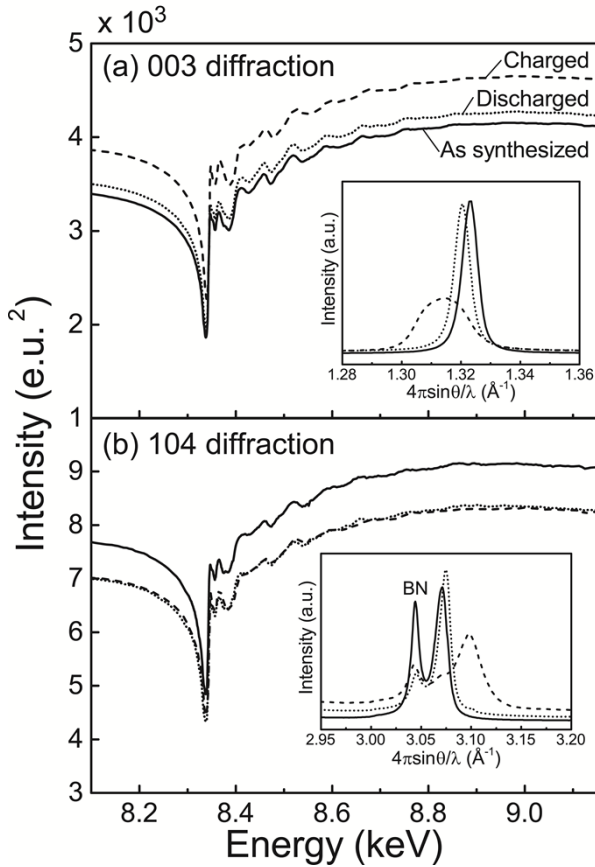


Figure S2. DAFS spectra of the (a) 003 diffraction and the (b) 104 diffraction. Solid, broken and dotted lines correspond to the as-synthesized, charged and discharged states, respectively. Insets show the peak profiles of each diffraction obtained at 8.007 keV.

DAFS spectra taken from the 003 and 104 diffractions at the different charge and discharge states are compared in Figs. S2a and S2b, respectively. All the spectra have local minima at the Ni K absorption edge of 8.33 keV, which is attributed to the significant contribution of  $f'$  in the complex atomic scattering factor of Ni:  $f(Q,E) = f^0(Q) + f'(E) + if''(E)$ , where  $Q$  is a scattering vector,  $E$  is the photon energy of the incident x-ray,  $f^0$  is a nonresonant term, and  $f'$  and  $f''$  are the real and imaginary contributions to the resonant terms, respectively. Furthermore,  $f''/E$  comparable to the

XAFS spectrum, including information about the local structures around Ni ions, was extracted from the measured DAFS spectra on the basis of the previously established LDR analysis technique.<sup>16</sup> Insets in Figs. S2a and S2b show the 003 and 104 XRD profiles, respectively, of each charge state; the profiles were collected at 8.007 keV.

## XANES simulations

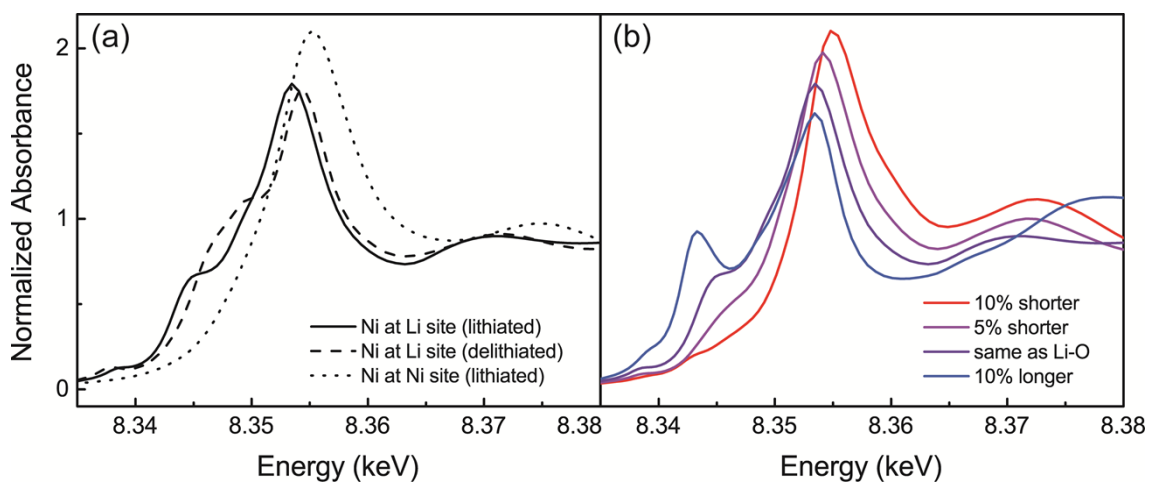


Figure S3. Simulated XANES spectra by FEFF 9.6 code. (a) The spectra of the Ni atoms at the Li site and Ni site with and without Li atoms. (b) The spectra of the interlayer Ni ( $\text{Ni}_{\text{Li}}$ ) with different bond lengths of  $\text{Ni}_{\text{Li}}\text{-O}$ .

The XANES simulations were performed using the FEFF 9.6 code<sup>36</sup> with self-consistent potential and RPA corehole. The crystalline model for the calculation of the interlayer Ni was constructed with a  $2 \times 2 \times 1$  ( $a \times b \times c$  in a hexagonal unit cell, respectively) supercell based on the structure parameters determined by Rietveld analysis of the as-synthesized sample by adding one Ni atom to the interlayer space. Structure models for the calculation of the bond-length dependence were produced by changing the coordination of the first-neighboring oxygen atoms while retaining the regular octahedron symmetry at the interlayer Ni site. Figure S3 (a) shows the site-dependency of the XANES spectra of Ni. The XANES spectrum at the interlayer Ni site without surrounding Li is also shown. The rise of the shoulder peak on the absorption edge can be clearly observed. Figure S3 (b) shows the bond-length dependence of the XANES spectra at

the interlayer Ni site. Increasing the bond length causes a significant increase in the intensity of the shoulder peak on the absorption edge, corresponding to the expansion of the interlayer space accompanying delithiation. In the experimental XANES spectrum, the significant evolution of the shoulder peak on the absorption edge was also observed; it was caused by the two factors described above: the absence of the surrounding Li and the increase in the bond lengths.

### Coordination environment of Ni at each site

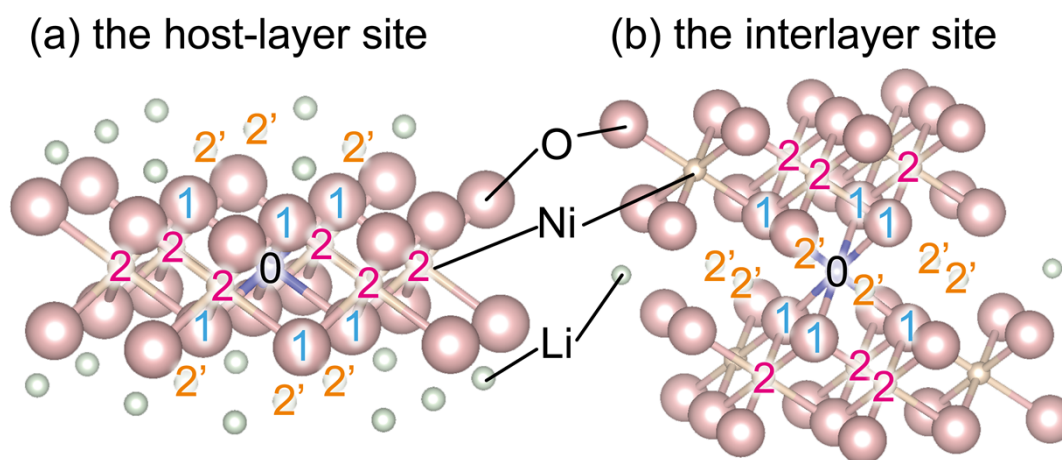


Figure S4. Coordination spheres at (a) the host-layer Ni ( $\text{Ni}_{\text{Ni}}$ ) and (b) the interlayer Ni ( $\text{Ni}_{\text{Li}}$ ) sites. The number 0 denotes the center atom. 1 and 2 (2') indicate the first and second coordination spheres, respectively.

Coordination spheres at the host-layer Ni and the interlayer Ni sites are shown in Fig. S4a and b, respectively. In both sites, the first neighboring atoms are six oxygen atoms (denoted 1), and the second neighboring atoms are six Li (2') and six Ni (2) atoms; however, the geometric positions differ. At the interlayer Ni site, six Ni atoms are located just above and below the interlayer space and six Li atoms are located in the same interlayer space. By contrast, at the original Ni site, six Ni atoms occupy the sample interlayer space and six Li atoms are located just above and below the interlayer space.